

**Magnetization study of  $\text{RuSr}_2\text{Y}_{1.5}\text{Ce}_{0.5}\text{Cu}_2\text{O}_{10}$** 

I. Felner

*Racah Institute of Physics, The Hebrew University, Jerusalem, 91904, Israel*

V. P. S. Awana

*National Physical Laboratory, K.S. Krishnan Marg, New Delhi 110012, India  
and Superconducting Materials Center, NIMS, 1-1 Namiki, Tsukuba, Ibaraki, 305 0044, Japan*

E. Takayama-Muromachi

*Superconducting Materials Center, NIMS, 1-1 Namiki, Tsukuba, Ibaraki, 305 0044, Japan*

(Received 17 March 2003; revised manuscript received 20 May 2003; published 16 September 2003)

We have studied the magnetic properties of nonsuperconducting  $\text{RuSr}_2L_{1.5}\text{Ce}_{0.5}\text{Cu}_2\text{O}_{10}$  [ $L = \text{Y}$ ,  $\text{Dy}$ , and  $\text{Ho}$  (Ru-1222)] compounds synthesized under high pressure (6 Gpa) at elevated temperature. These materials become magnetically ordered at  $T_M = 152(2)$  K regardless of  $L$ . The wide ferromagneticlike hysteresis loops, which open at 5 K, close themselves around  $T_{\text{irr}} = 90\text{--}100$  K and the remanent magnetizations ( $M_{\text{rem}}$ ) and coercive fields ( $H_C$ ) become zero. Surprisingly, at  $T_{\text{irr}} < T < T_M$  a reappearance of the  $M_{\text{rem}}$  and  $H_C$  (with a peak at 120–130 K) is observed for all three samples studied. For the nonmagnetic  $L = \text{Y}$  compound, the extracted ferromagnetic moment is at 5 K and the effective paramagnetic moments are  $0.75$  and  $2.05\mu_B/\text{Ru}$ , values which are close to the expected  $1\mu_B$  and  $1.73\mu_B$ , respectively, for the low-spin state of  $\text{Ru}^{5+}$ . We argue that the Ru-1222 system becomes: (i) antiferromagnetically ordered at  $T_M$  and in this range a metamagnetic transition is induced by the external field. (ii) At  $T_{\text{irr}} < T_M$ , weak ferromagnetism is induced by the canting of the Ru moments.

DOI: 10.1103/PhysRevB.68.094508

PACS number(s): 74.10.+v, 74.25.Ha

**I. INTRODUCTION**

The interplay of magnetism and superconductivity (SC) is a fundamental problem in condensed-matter physics and has been studied experimentally and theoretically for almost four decades. Coexistence of weak ferromagnetism and SC was discovered a few years ago in  $\text{RuSr}_2L_{2-x}\text{Ce}_x\text{Cu}_2\text{O}_{10}$  [ $L = \text{Eu}$  and  $\text{Gd}$  (Ru-1222)] layered cuprate systems,<sup>1,2</sup> and more recently<sup>3</sup> in  $\text{RuSr}_2\text{GdCu}_2\text{O}_8$  (Ru-1212). The SC charge carriers originate from the  $\text{CuO}_2$  planes and the weak-ferromagnetic (W-FM) state is confined to the Ru layers. In both systems, the magnetic order does not vanish when SC sets in at  $T_C$ , but remains unchanged and coexists with the SC state. The Ru-1222 materials (for  $L = \text{Eu}$  and  $\text{Gd}$ ) display a magnetic transition at  $T_M = 125\text{--}180$  K and bulk SC below  $T_C = 32\text{--}50$  K ( $T_M > T_C$ ) depending on oxygen concentration and sample preparation.<sup>1</sup> The hole doping of the Cu-O planes, which results in metallic behavior and SC, can be optimized with appropriate variation of the Ru/Ce ratio.<sup>4</sup> SC occurs for Ce contents of 0.4–0.8, and the highest  $T_C$  was obtained for Ce=0.6. SC survives because the Ru magnetic moments probably align in the basal planes, which are practically decoupled from the  $\text{CuO}_2$  planes, so that there is no pair breaking. X-ray-absorption spectroscopy (XAS), taken at the  $K$  edge of Ru, at room temperature reveals that the Ru ions are basically  $\text{Ru}^{5+}$  or  $\text{Ru}^{4.75+}$  (see Ref. 6). Ru remains pentavalent irrespective of the Ce concentration, which means that there is no charge transfer to the Ru-O layers with increasing Ce concentration.<sup>7</sup> The remaining unresolved question is whether the  $\text{Ru}^{5+}$  in Ru-1222 is in its low- ( $S = 1/2$ ) or high- ( $S = 3/2$ ) spin state. It is also apparent that bulk SC only appears in iso-structural  $\text{MSr}_2L_{2-x}\text{Ce}_x\text{Cu}_2\text{O}_{10}$

( $M = \text{Nb}$  and  $\text{Ta}$ ) with  $T_C \sim 28\text{--}30$  K, in which the  $M$  ions are pentavalent.<sup>8</sup>

The SC state in Ru-1222 is well established and understandable. Specific-heat studies show a sizable typical jump at  $T_C$  and the magnitude of the  $\Delta C/T$  ( $0.08$  mJ/gK<sup>2</sup>) clearly indicates the presence of bulk SC.<sup>9</sup> The specific-heat anomaly is independent of the applied magnetic field. The temperature dependence of the magnetoresistance data<sup>10</sup> yields an upper critical field of  $H_{c2}(0) = 39$  T and a coherence length of  $\zeta(0) = 140$  Å along the  $\text{CuO}_2$  planes. Due to the granular nature of the materials the critical current density at 5 K is extremely small [ $J_C(0) = 22$  A/cm<sup>2</sup>] as compared to other high- $T_C$  superconducting materials.<sup>11</sup> Below  $T_C$ , the magnetoresistance  $\Delta R(H) = R(H) - R(0)$  is positive and unexpected hysteresis loops are observed.  $\Delta R(H)$  on decreasing the applied field ( $H$ ) is much smaller than  $\Delta R(H)$  for increasing  $H$ . The width of the loops depends strongly on the weak-link properties. Similar hysteresis loops are observed in superconductive, nonmagnetic Nb-1222 ( $T_C = 28$  K), thus eliminating the possibility that the hysteresis phenomenon is caused by the coexistence of SC and magnetic states.<sup>11</sup> Scanning tunneling spectroscopy<sup>1</sup> and magneto-optic experiments<sup>12</sup> have demonstrated that all materials are microscopically uniform with no evidence for spatial phase separation of SC and magnetic regions. That is, both states coexist intrinsically on the microscopic scale. Studies of Zn substitution for Cu in oxygen-annealed  $\text{RuSr}_2\text{Eu}_{2-x}\text{Ce}_x(\text{Cu}_{1-x}\text{Zn}_x)_2\text{O}_{10}$  ( $x = 0, 0.01, \text{ and } 0.025$ ) reveal that Zn reduces  $T_C$  from  $T_C = 38$  K for  $x = 0$  to 26 K for 0.01 and that for  $x = 0.025$ , the material is not superconductive down to 4.2 K. On the other hand, the magnetic state of

the Ru sublattice is not effected by the presence or absence of the superconductive state, indicating that the two states are practically decoupled.<sup>13</sup>

One of the most disputed questions is that of the magnetic structure of Ru-1222. In contrast to the Ru-1212 system in which the antiferromagnetic (AFM) nature of the Ru sublattice has been determined by neutron-diffraction studies,<sup>14,15</sup> the detailed magnetic features of the Ru-1222 system are lacking. The accumulated results are compatible with two alternative models, both of which are used for understanding the qualitative features at low applied fields. (A) Going from high to low temperatures, the magnetic behavior is basically divided into two regions.<sup>4</sup> (i) Depending on Ce content, at  $T_M$ , all the material becomes antiferromagnetically ordered. (ii) At  $T_{irr} (< T_M)$ , a W-FM state is induced, which originates from canting of the Ru moments. This canting is probably a result of the tilting of the  $\text{RuO}_6$  octahedra from the crystallographic  $c$  axis,<sup>16</sup> which causes the adjacent spins to cant out of their original AFM direction and to align a component of the moments with the direction of the applied field. At  $T_C < T_{irr}$ , SC is induced and both the superconductive and the W-FM states coexist intrinsically on a microscopic scale. (B) Detailed analysis of the magnetization under various thermal-magnetic conditions suggests a *magnetic* phase separation of Ru-1222 into FM and AFM (Ref. 17) nanodomain species inside the crystal grains. A minor part of the material becomes ferromagnetic (FM) at  $T_M$ , whereas the major part orders antiferromagnetically at a lower temperature and becomes superconductive at  $T_C$ . In this scenario, the unusual SC state is well understood.

In attempting to understand the W-FM state in Ru-1222, we report here a detailed magnetization study of  $\text{RuSr}_2\text{Y}_{1.5}\text{Ce}_{0.5}\text{Cu}_2\text{O}_{10}$  (Ru-1222Y) which has been synthesized at 6 GPa at 1200 °C.<sup>18</sup> Nonmagnetic Y has replaced the magnetic Eu and/or Gd ions and permits an easier direct interpretation of the intrinsic Ru magnetism. The results are compared to the data obtained for  $\text{RuSr}_2\text{Dy}_{1.5}\text{Ce}_{0.5}\text{Cu}_2\text{O}_{10}$  (Ru-1222Dy) and  $\text{RuSr}_2\text{Ho}_{1.5}\text{Ce}_{0.5}\text{Cu}_2\text{O}_{10}$  (Ru-1222Ho) both synthesized under the same conditions.<sup>18</sup> We show below that the magnetic structure of all samples studied can be interpreted only by assuming model (A) discussed above. None of the samples described here is superconducting. Attempts to induce SC by annealing the materials under high oxygen pressure at elevated temperatures have failed.

## II. EXPERIMENTAL DETAILS

Ceramic samples with the nominal composition  $\text{RuSr}_2\text{L}_{1.5}\text{Ce}_{0.5}\text{Cu}_2\text{O}_{10}$  ( $L = \text{Y, Dy, and Ho}$ ) under 6 GPa at 1200 °C for 2 h were prepared by a solid-state reaction technique as described in Ref. 18. Determination of the absolute oxygen content in these materials is difficult because  $\text{CeO}_2$  is not completely reducible to a stoichiometric oxide when heated to high temperatures. Powder x-ray-diffraction (XRD) measurements confirmed the tetragonal structure (space group  $I4/mmm$ ) and yield the lattice parameters  $a = 3.824(1), 3.819(1), \text{ and } 3.813(1) \text{ \AA}$  and  $c = 28.445, 28.439(1), \text{ and } 28.419(1) \text{ \AA}$  for  $L = \text{Dy, Y, and Ho}$ , respectively. Ru-1222Dy and Ru-1222Ho are single-phase materi-

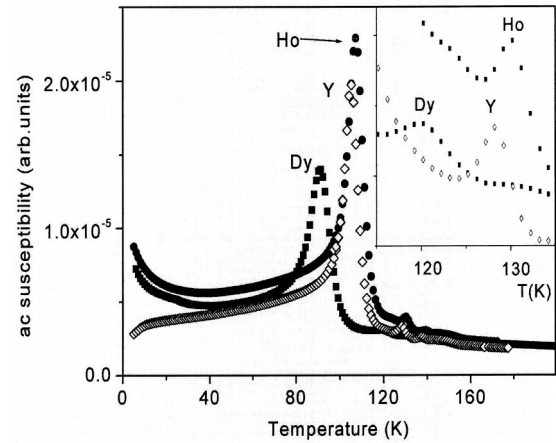


FIG. 1. The real part of the ac susceptibility of  $\text{RuSr}_2\text{L}_{1.5}\text{Ce}_{0.5}\text{Cu}_2\text{O}_{10}$ .

als, whereas the Ru-1222Y pattern shows three small (less than 3%) unidentified extra peaks.<sup>18</sup> Zero-field-cooled (ZFC) and field-cooled (FC) dc magnetic measurements at various applied field in the range of 5–300 K were performed in a commercial (Quantum Design) super-conducting quantum interference device (SQUID) magnetometer. ac susceptibility was measured (at  $H_{dc} = 0$ ) by a homemade probe, with excitation frequency and amplitude of 733 Hz and 30 mOe, respectively, inserted into the SQUID magnetometer.

## III. EXPERIMENTAL RESULTS

In contrast to the magnetosuperconducting  $\text{RuSr}_2\text{L}_{1.5}\text{Ce}_{0.5}\text{Cu}_2\text{O}_{10}$  ( $L = \text{Eu and Gd}$ ), obtained at ambient pressure, the heavy nonsuperconducting  $L$  (and Y) materials can be synthesized only under high pressures. The samples obtained are insulating materials down to 5 K. The rapid increase in the resistivity with decreasing temperature (not shown) can be characterized by fitting the data to  $R\alpha 10^{-bT}$  where  $b$  is of the order 0.02. Attempts to induce SC by annealing the Ru-1222Y material under 75-atm oxygen at 800 °C for 6 h leads to decomposition into a  $\text{RuSr}_2\text{YO}_6$  (1216) phase.<sup>19</sup> The ionic radius of  $\text{Dy}^{3+}$  is 0.91 Å as compared to 0.90 Å for both  $\text{Y}^{3+}$  and  $\text{Ho}^{3+}$  ions. Therefore the unit-cell volume ( $V$ ) of  $\text{RuSr}_2\text{Dy}_{1.5}\text{Ce}_{0.5}\text{Cu}_2\text{O}_{10}$  ( $415.9 \text{ \AA}^3$ ), is a bit larger than those of  $L = \text{Y}$  and  $\text{Ho}$ ,  $414.7 \text{ \AA}^3$  and  $413.2 \text{ \AA}^3$ , respectively.

The temperature dependence of the normalized real ac susceptibility for the  $\text{RuSr}_2\text{L}_{1.5}\text{Ce}_{0.5}\text{Cu}_2\text{O}_{10}$  system is presented in Fig. 1. It is readily observed that none of the materials are superconductive down to 4.2 K. The two peaks observed, namely, the major one at 91(1), 105(1), and 107(1) K, and the minor one (Fig. 1, inset) at  $T = 120(1), 128(1), \text{ and } 130(1) \text{ K}$ , for  $L = \text{Dy, Y, and Ho}$ , respectively, are both inversely proportional to  $V$  listed above. The increase of the signals below 40 K for  $L = \text{Dy and Ho}$  is related to their large paramagnetic (PM) contribution at low temperatures. Neither of the two peaks is the magnetic transition  $T_M(\text{Ru})$  of the system, as discussed below. Beside these differences, the magnetic behavior of all three samples is simi-

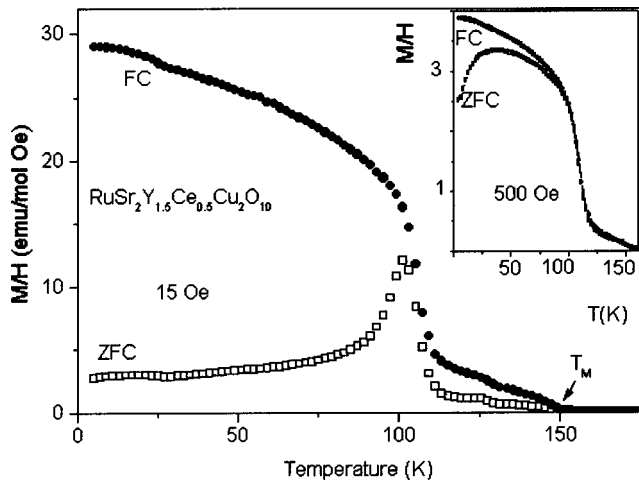


FIG. 2. ZFC and FC  $M/H$  for Ru-1222Y measured at 15 Oe and 500 Oe (inset).

lar and for the sake of brevity we describe in detail the magnetic properties of Ru-1222Y in which Y is not magnetic. In that sense, the present  $\text{RuSr}_2\text{Y}_{1.5}\text{Ce}_{0.5}\text{Cu}_2\text{O}_{10}$  system resembles the nonsuperconductive  $\text{RuSr}_2\text{EuCeCu}_2\text{O}_{10}$  material discussed in Ref. 4.

ZFC and FC dc magnetic measurements were performed over a broad range of applied magnetic fields, and typical  $M/H$  curves for Ru-1222Y measured at 15 (and 500 Oe) are shown in Fig. 2. The two curves merge twice, at  $T_{\text{irr}} = 105(2)$  K and at  $T_M(\text{Ru}) = 152(1)$  K. Note (i) the small peak in the ZFC branch around 125 K [this peak and  $T_{\text{irr}}$  fit well with the minor and major peaks of the ac susceptibility (Fig. 1)], and (b) the ferromagneticlike shape of the FC branches. In general, the ZFC/FC curves do not lend themselves to an easy determination of  $T_M(\text{Ru})$ , and  $T_M(\text{Ru})$  was obtained directly from the temperature dependence of the spontaneous moment ( $M_s$ ).<sup>1</sup> Here, since Y is a nonmagnetic ion, the  $M/H(T)$  curve, measured at low  $H$ , permits a direct determination of  $T_M(\text{Ru})$ . At 500 Oe the ZFC and FC branches merge also at  $T_{\text{irr}}$  (Fig. 2, inset), in contrast to previous measurements on magnetic  $L$  ions,<sup>1</sup> in which  $T_{\text{irr}}$  is field dependent and shifts to lower temperatures with  $H$ . The irreversibility is washed out for  $H = 2.5$  kOe and both ZFC and FC curves collapse into a single FM-like behavior.

Isothermal  $M(H)$  measurements (up to 50 kOe) at various temperatures have been carried out, and the results obtained are shown in Figs. 3 and 4. Below  $T_M$ , all  $M(H)$  curves depend strongly on  $H$  (up to  $\sim 1-4$  kOe), until a common slope is reached. The remarkable feature shown in Fig. 3 is the apparent tendency toward saturation at 5 K, but not reaching full saturation even at 50 kOe. Similar behavior was observed in  $\text{RuSr}_2\text{YCu}_2\text{O}_8$ .<sup>20</sup> This phenomenon is typical of itinerant ferromagnetic materials and reminiscence of the unsaturated  $M(H)$  curves observed for itinerant ferromagnetic  $\text{SrRuO}_3$  single crystals at various orientations.<sup>21</sup> The moment at 5 K and 50 kOe is  $M = 0.71\mu_B/\text{Ru}$  (Fig. 3). Estimation of the Ru moment at infinite  $H$ , by plotting  $M^2 \propto 1/H$  (for high  $H$  values), and extrapolating to  $1/H = 0$ , yields  $M_{\text{max}} = 0.75\mu_B/\text{Ru}$ , a value which is smaller than  $g\mu_B S = 1\mu_B$ ,

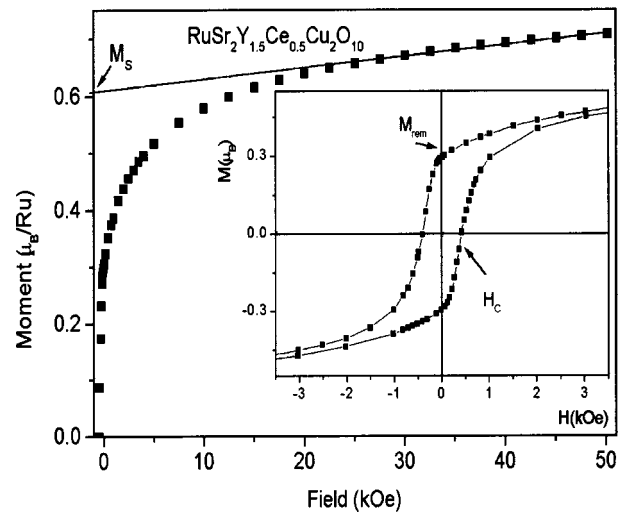


FIG. 3. The isothermal magnetization at 5 K and the ferromagneticlike hysteresis loop (inset).

the expected saturation moment for  $\text{Ru}^{5+}$  in the low-spin state ( $g = 2$  and  $S = 0.5$ ).

The linear part of  $M(H)$  in Fig. 3 can be described as  $M(H) = M_s + \chi H$ , where  $M_s = 0.63(1)\mu_B$  is the value obtained by the extrapolation to  $H = 0$ , and  $\chi = dM/dH$  is the slope ( $8.5 \times 10^{-3} \text{ emu/mol Oe} = 1.53 \times 10^{-2} \mu_B/T$ ). This  $\chi$  is much larger than the Cu-ion contribution to the susceptibility discussed below. Similar  $M(H)$  curves have been measured at various temperatures and Fig. 5 shows the temperature dependence of  $M_s$ . The extrapolated  $M_s$  at zero yields  $T_M(\text{Ru}) = 152(2)$  K exactly as obtained in Fig. 2. A similar procedure for the magnetic  $L = \text{Dy}$  and  $\text{Ho}$  ions yields 150(1) K for both materials, indicating that, within the uncertainty limit,  $T_M(\text{Ru})$  remains constant regardless of  $L$ . [The small tail above  $T_M$  which appears only for  $L = \text{Y}$ , is probably due to the presence of a small amount of  $\text{SrRuO}_3$  (not detectable by XRD)]. The slope  $\chi = M/H$  obtained at various temperatures is exhibited in Fig. 6. It appears that  $\chi$  does not change much up to  $T_{\text{irr}}$ , and then rises up to  $T_M(\text{Ru})$ . Above this temperature the slope follows the Curie-Weiss law discussed below.

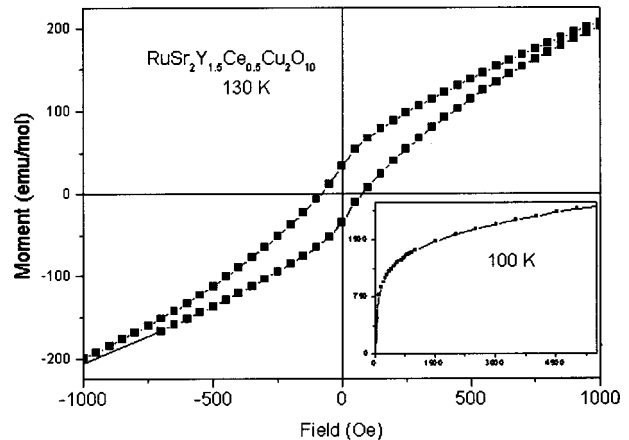


FIG. 4. The hysteresis loop opens at 130 K and the magnetization at 100 K (inset).

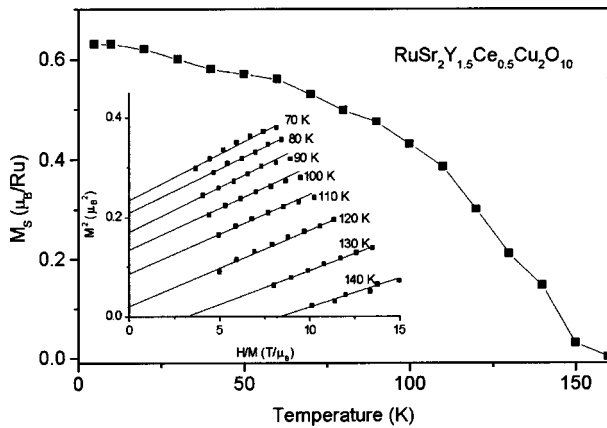


FIG. 5. The temperature dependence of the saturation moment of R-1222Y. The Arrott plots are shown in the inset.

At low applied fields, the  $M(H)$  curve exhibits a typical ferromagneticlike hysteresis loop (Fig. 3, inset) similar to that reported in Refs. 1–4. Two other characteristic parameters of the hysteresis loops at 5 K are shown in Fig. 3 (inset), namely, the remnant moment ( $M_{\text{rem}}=0.31 \mu_B/\text{Ru}$ ) and the coercive field ( $H_C=410$  Oe). [For  $L=\text{Dy}$  and  $\text{Ho}$  at 5 K we obtained  $M_{\text{rem}}=0.30$  and  $0.41 \mu_B/\text{Ru}$  and  $H_C=470$  and  $320$  Oe, respectively]. The  $M_{\text{rem}}(T)$  and  $H_C(T)$  values are shown in Fig. 7. Both  $M_{\text{rem}}(T)$  and  $H_C(T)$  become zero around 100 K which means that essentially no discernible hysteresis is observed at  $T_{\text{irr}}$  (Fig. 4, inset). Surprisingly, at higher temperatures, reappearance of the hysteresis loops is obtained (Fig. 4) with a peak at 120 K for  $M_{\text{rem}}(T)$  and  $H_C(T)$  (Fig. 7, inset) close to the peaks observed in Figs. 1 and 2. In contrast to the FM-like hysteresis loop obtained at  $T < T_{\text{irr}}$  (Fig. 3, inset), the loops above  $T_{\text{irr}}$  exhibit an AFM-like feature. Similar behavior is observed for Ru-1222Dy (Fig. 8) and for Ru-1222Ho.<sup>18</sup>

Above  $T_M(\text{Ru})$ , the  $\chi(T)$  curve for  $\text{RuSr}_2\text{Y}_{1.5}\text{Ce}_{0.5}\text{Cu}_2\text{O}_{10}$ , measured at 20 kOe up to 400 K, has the typical PM shape and can be fitted by the Curie-Weiss (CW) law:  $\chi=\chi_0+C/(T-\theta)$ , where  $\chi_0$  is the temperature-independent part of  $\chi$ ,  $C$  is the Curie constant,

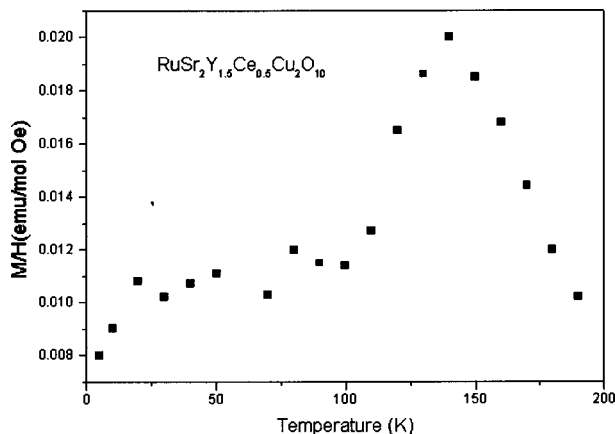


FIG. 6. The slope of the high-field values, at various temperatures.

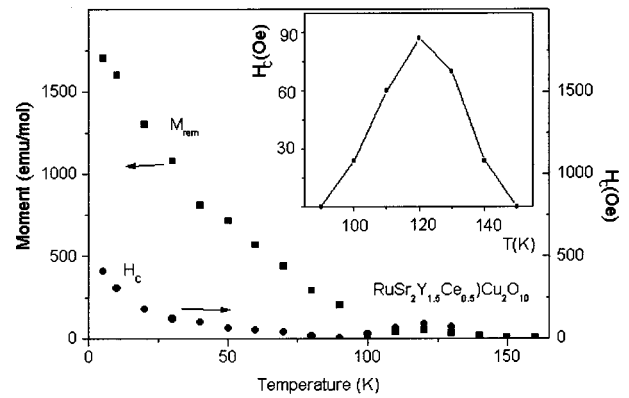


FIG. 7. The temperature dependence of the remnant and coercive field of R-1222Y.

and  $\theta$  is the CW temperature. In order to isolate the Ru intrinsic magnetic contribution, we also measured (up to 350 K at 20 kOe)  $\chi(T)$  of  $\text{YBa}_2\text{Cu}_3\text{O}_7$  which is roughly temperature independent ( $1.8-2 \times 10^{-4}$  emu/mol Oe) with values which are two orders of magnitude lower than  $\chi(T)$  of Ru-1222Y. After subtracting  $2/3\chi(T)$  of  $\text{YBa}_2\text{Cu}_3\text{O}_7$  from the measured  $\chi(T)$  of Ru-1222Y, we obtained  $\chi_0=0.0014$  emu/mol Oe,  $C=0.523(1)$  emu K/mol Oe, and  $\theta=136(1)$  K, which corresponds to  $P_{\text{eff}}=2.05 \mu_B/\text{Ru}$ . (In fact, similar values were obtained for the fit of the raw data.) This  $\chi_0$  is comparable to  $\chi_0$  of Ru-1212,<sup>20</sup> and  $\theta=136$  K is in fair agreement with  $T_M(\text{Ru})=152$  K extracted from Figs. 2 and 5.  $P_{\text{eff}}=2.05 \mu_B$  is somewhat greater than  $1.73 \mu_B$ , the expected value of the low-spin state of  $\text{Ru}^{5+}$  and it is in fair agreement with  $P_{\text{eff}}=2.13 \mu_B$  obtained in Ref. 4 for  $\text{RuSr}_2\text{Eu}_{1.5}\text{Ce}_{0.5}\text{Cu}_2\text{O}_{10}$ , where  $P_{\text{eff}}(\text{Ru})$  was obtained by carefully subtracting all extra contributions to  $\chi(T)$ . In any case, this  $P_{\text{eff}}$  is much smaller than  $2.8 \mu_B/\text{Ru}$  reported for R-1222Eu.<sup>22</sup> [ $\chi(T)$  for  $L=\text{Dy}$  and  $\text{Ho}$  adheres closely to the CW law and the values of  $C$  obtained are 15.6 and 12.1 emu K/mol Oe, respectively. These values are much smaller than the theoretical values expected for  $\text{Dy}^{3+}$  and  $\text{Ho}^{3+}$  free ions, probably due to strong crystal-field effects. However, this is of a little interest in the present discussion.]

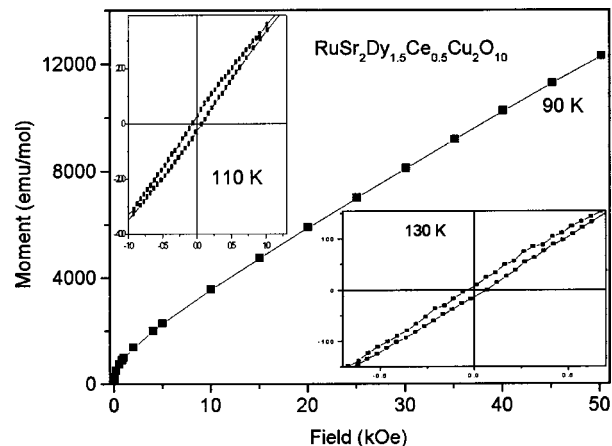


FIG. 8. The isothermal magnetization curves for R-1222Dy at 90, 110, and 130 K. Note the absence of hysteresis at 90 K.

#### IV. DISCUSSION

In a recent paper<sup>3</sup> we have shown that a small amount (2.5 at. %) of Zn suppresses completely the SC state in  $\text{RuSr}_2\text{Eu}_{2-x}\text{Ce}_x(\text{Cu}_{1-x}\text{Zn}_x)_2\text{O}_{10}$  and that the magnetic properties of the Ru sublattice are not effected by the presence or the absence of this SC state. Our general picture is that (i) in the Ru-1222 system, all compounds have a similar magnetic structure and (ii) the two states are practically decoupled. Therefore, the study of nonsuperconductive and nonmagnetic Y ions permits an easier interpretation of the intrinsic Ru-O sublattice magnetism, in particular, that of the PM state.

##### A. The qualitative magnetic structure of $\text{RuSr}_2\text{Y}_{1.5}\text{Ce}_{0.5}\text{Cu}_2\text{O}_{10}$ .

While our data described here do not include any determination of the magnetic structure of the Ru sublattice, the results are compatible with a simple model, which is, however, of use in understanding the qualitative features at low applied fields. Starting from high to low temperatures, the magnetic behavior is basically divided into four regions.

(i) At elevated temperatures, the paramagnetic net Ru moment is well described by the CW law, and the extracted values for Ru-1222Y are  $P_{\text{eff}}=2.05\mu_B$  and  $\theta=136$  K. This  $P_{\text{eff}}$  is somewhat greater than  $1.73\mu_B$ , the calculated value of  $\text{Ru}^{5+}$  in the low-spin state, and suggests that the assumption of completely localized moments is not adequate for this system.

(ii) At  $T_M(=152$  K), the Ru sublattice becomes basically antiferromagnetically ordered at low applied fields. This interpretation is supported by the small peaks observed in the ac susceptibility (Fig. 1) and in the ZFC branch when measured at low fields (Fig. 2). At higher applied fields a metamagnetic transition is induced. In general, metamagnetism in insulating AFM systems refers to the magnetic transition produced by an external  $H$ , when the strength of the field equals or exceeds the exchange coupling between the magnetic moments. In Ru-1222Y, the AFM Ru moments are realigned through a spin-flip process by  $H$ , to form the AFM-like-shape hysteresis loops observed in Figs. 4 and 8. Note the difference between the AFM-like and the FM-like (Fig. 3) hysteresis loops.

(iii) Around  $T_{\text{irr}}=100$  K a ferromagneticlike shape of the FC branches is observed (Fig. 2).  $T_{\text{irr}}$  is defined as the merging point of the low-field ZFC and FC branches, or alternatively, at the temperature in which  $M_{\text{rem}}$  and  $H_C$  first disappear. The exact structure of the Ru spin ordering below  $T_{\text{irr}}$  is still debated and no conclusions have been reached as yet. Neutron-diffraction measurements are required to precisely determine the nature of the magnetic order. Without these measurements, we may assume three scenarios for the magnetic behavior in this region as follows. (I) Our preferred scenario is that at  $T_{\text{irr}}$  a weak ferromagnetism is induced, which originates from canting of the Ru moments. The saturation moment of  $\text{Ru}^{5+}$  in the low-spin state is  $1\mu_B/\text{Ru}$  ( $3\mu_B/\text{Ru}$  for  $\text{Ru}^{5+}$  in the high-spin state). We note that  $M_{\text{max}}=0.75\mu_B/\text{Ru}$  obtained at 5 K is a large fraction of  $1\mu_B$ , implying a very large canting angle ( $49^\circ$ ) of the AFM Ru moments. The ratio of  $M_{\text{rem}}/M_{\text{max}}$  ( $0.31/0.75=0.41$ ) and

the positive  $\theta=136$  K are also consistent with this W-FM interpretation. (II) Alternatively, a frequency-dependence cusp was observed in the ac susceptibility of Ru-1222, which may be interpreted as a spin-glass behavior.<sup>23</sup> A spin glass is a collection of magnetic moments whose state is frozen and disordered. To produce such a state, two ingredients are necessary: frustration and partial randomness of interaction between the magnetic moments. Although Ru ions in Ru-1222 are arranged in a strictly periodic order, it is possible that the incomplete oxygen stoichiometry and/or the small distortion of the oxygen octahedra<sup>16</sup> are involved in inducing frustration, which, in turn leads to glassy behavior. (III) The unsaturated  $M(H)$  curve at low temperatures may suggest (similar to  $\text{SrRuO}_3$ ) itinerant electron magnetism in this system. Consequently, we used the conventional so-called Arrott plots to determine the magnetic transition. In Fig. 5 (inset) we have plotted the field values of Ru-1222Y at various temperatures and the magnetic transition extracted is 125(3) K, midway between  $T_{\text{irr}}$  and  $T_M$ . Supporting evidence to this third scenario are the high  $P_{\text{eff}}/M_{\text{sat}}\sim 3$  ratio and the  $P_{\text{eff}}=2.05\mu_B$  value, which exceeds the expected value for a localized  $\text{Ru}^{5+}$  low-spin state.

(iv) For  $L=\text{Eu}$  and  $\text{Gd}$ , SC is induced at  $T_C$ .  $T_C<T_M$  depends strongly on Ce (as a hole carrier) and on oxygen concentrations.<sup>1-5</sup> Below  $T_C$ , both SC and weak-ferromagnetic states coexist and the two states are practically decoupled.<sup>13</sup>

We think that the magnetic behavior of Ru-1222Y can be interpreted only by assuming model (A) regardless of the magnetic features of region (iii). The data described here exclude the magnetic AFM and FM phase-separation model<sup>17</sup> (B) discussed above. According to this model, a minor part (10%) of the material becomes FM at  $T_M$  and this FM fraction persists down to low temperatures. At  $T_{\text{irr}}$ , the major part of the material orders antiferromagnetically and this part only becomes superconductive at  $T_C$ . In this scenario, the unusual SC state is well understood. Thus, below  $T_{\text{irr}}$ , the Ru-1222 materials are in fact a mixture of both FM and AFM phases. However, model (B) cannot be reconciled with the accumulated data presented here: (i) the high  $0.75\mu_B/\text{Ru}$  moment at 5 K and (ii) the continuous  $M_s$  curve (Fig. 5), which does not show any inflection at  $T_{\text{irr}}$  or at lower temperatures, (iii) the high positive  $\theta$  value, (iv) the peaks in both ac and dc magnetization curves which indicate an AFM ordering above  $T_{\text{irr}}$ , and (v) the reopening of hysteresis loops above 100 K, which as a result, increases both  $M_{\text{rem}}$  and  $H_C$  (Fig. 7). According to model (B), the hysteresis loops opened at  $T_M$  would remain all the way down to low temperatures and both  $M_{\text{rem}}$  and  $H_C$  would increase continuously, or at least remain constant. Additional data include (vi) the different shape of the hysteresis loops observed below and above  $T_{\text{irr}}$ .

As a final point of interest we compare all of the magnetic behavior of Ru-1222Y to that of ferromagnetic  $\text{La}(\text{Fe}_x\text{Si}_{1-x})_{13}$  intermetallic compounds.<sup>24</sup> In both systems above the FM transition (or W-FM transition in Ru-1222), small hysteresis loops are opened and both systems exhibit meta-magnetic transitions. In  $\text{La}(\text{Fe}_x\text{Si}_{1-x})_{13}$ , the itinerant

electron metamagnetic transition observed above the FM transition ( $T_{FM}$ ) is a result of thermal activations that make the FM energy minimum shallower than the PM one, resulting in the PM state above  $T_{FM}$ . By applying a field, the FM energy minimum again becomes lower than the PM one and a metamagnetic transition from the PM to the itinerant FM state is induced. As a result small hysteresis loops are observed above  $T_{FM}$ . The single difference is that in the Ru-1222 system, the ground state in region (ii) is AFM and the external  $H$  induces a spin-flip transition.

## V. CONCLUSION

The magnetic behavior of all non-superconducting materials studied is practically the same, and the magnetic parameters, such as  $T_{irr}$ ,  $T_M$ ,  $H_C$ , and  $M_{sat}$ , are similar. Two steps in the magnetic behavior are presented. At  $T_M=152(2)$  K all

materials become antiferromagnetically ordered, a metamagnetic transition is induced by the applied field, and typical AFM hysteresis loops are observed. At  $T_{irr}$  ranging from 90 to 100 K, a W-FM state is induced, originating from canting of Ru moments. The maximum moment at 5 K is 75% of the expected value for  $Ru^{5+}$ , indicating a W-FM state below  $T_{irr}$ . The PM parameters extracted indicate that Ru is pentavalent in the low-spin state. The present results exclude the proposed magnetic phase-separation model in the Ru-1222 system.

## ACKNOWLEDGMENTS

We are grateful to E. Galstyan for assistance in the ac measurements. This research was supported by the Israel Academy of Science and Technology and by the Klachky Foundation for Superconductivity.

- 
- <sup>1</sup>I. Felner, U. Asaf, Y. Levi, and O. Millo, Phys. Rev. B **55**, R3374 (1997); Physica C **334**, 141 (2000).  
<sup>2</sup>Y.Y. Xue, B. Lorenz, A. Baikalov, D.H. Cao, Z.G. Li, and C.W. Chu, Phys. Rev. B **66**, 014503 (2002); Y.Y. Xue, D.H. Cao, B. Lorenz, and C.W. Chu, *ibid.* **65**, 020511(R) (2002).  
<sup>3</sup>C. Bernhard, J.L. Tallon, Ch. Niedermayer, Th. Blasius, A. Golnik, B. Ttucher, R.K. Kremer, and E.J. Ansaldo, Phys. Rev. B **59**, 14 099 (1999).  
<sup>4</sup>I. Felner, U. Asaf, and E. Galstyan, Phys. Rev. B **66**, 024503 (2002).  
<sup>5</sup>I. Felner, U. Asaf, C. Godart, and E. Alleno, Physica B **259–261**, 703 (1999).  
<sup>6</sup>V.P.S. Awana, M. Karppinen, H. Yamauchi, R.S. Liu, J.M. Chen, and L.-Y. Jang, J. Low Temp. Phys. **131**, 1211 (2003).  
<sup>7</sup>G.V.M. Williams, L.Y. Jang, and R.S. Liu, Phys. Rev. B **65**, 064508 (2002).  
<sup>8</sup>R.J. Cava, J.J. Krajewski, H. Takagi, H. Zandbergen, R.W.R.B. Van Dover, W.F. Peck, Jr., and B. Hessen, Physica C **191**, 237 (1992).  
<sup>9</sup>X.H. Chen, Z. Sun, K. Q. Wang, S.Y. Li, Y.M. Xiong, M. Yu, and L.Z. Cao, Phys. Rev. B **63**, 064506 (2001).  
<sup>10</sup>M.T. Escote, V.A. Meza, R.F. Jardim, L. Ben-Dor, M.S. Torikachvili, and A.H. Lacerda, Phys. Rev. B **66**, 144503 (2002).  
<sup>11</sup>I. Felner, E. Galstyan, B. Lorenz, D. Cao, Y.S. Wang, Y.Y. Xue, and C.W. Chu, Phys. Rev. B **67**, 134506 (2003).  
<sup>12</sup>M. Shigemori, T. Matci, N. Koshizuka, I. Felner, and M. Abe, Ferrites Proc. ICF **8**, 287 (2000).  
<sup>13</sup>I. Felner and E. Galstyan, Int. J. Mod. Phys. B (to be published).  
<sup>14</sup>J.W. Lynn, B. Keimer, C. Ulrich, C. Bernhard, and J.L. Tallon, Phys. Rev. B **61**, R14 964 (2000).  
<sup>15</sup>J.D. Jorgensen, O. Chmaissem, H. Shaked, S. Short, P.W. Klamut, B. Dabrowski, and J.L. Tallon, Phys. Rev. B **63**, 054440 (2001).  
<sup>16</sup>C.S. Knee, B.D. Rainford, and M.T. Weller, J. Mater. Chem. **10**, 2445 (2000).  
<sup>17</sup>Y.Y. Xue, D.H. Cao, B. Lorenz, and C.W. Chu, Phys. Rev. B **65**, 020511(R) (2002).  
<sup>18</sup>V.P.S. Awana and E. Takayama-Muromachii, Physica C **390**, 101 (2003).  
<sup>19</sup>I.I. Nowik, I. Felner, and U. Asaf, Hyperfine Interact. **213–217**, 213 (2002).  
<sup>20</sup>H. Takagiwa, J. Akimitso, H.K. Furukawa, and H. Yoshizawa, J. Phys. Soc. Jpn. **70**, 333 (2001).  
<sup>21</sup>G. Cao, S. McCall, M. Shepard, J.E. Crow, and R.P. Guretin, Phys. Rev. B **56**, 321 (1997).  
<sup>22</sup>A. Butera, M. V. Mansilla, A. Fainstein, and G.V.M. Williams, Physica B **320**, 316 (2002).  
<sup>23</sup>C.A. Cardoso, F.M. Araujo-Moreira, V.P.S. Awana, E. Takayama-Muromachi, O.F. de Lima, H. Yamauchi, and M. Karppinen, Phys. Rev. B **67**, 020407 (2003).  
<sup>24</sup>F. Fujita, Y. Akamatsu, and K. Fukamichi, J. Appl. Phys. **85**, 4756 (1999).